Microstructure evolution and diffusion of ruthenium in silicon carbide, and the implications for structural integrity of SiC layer in TRISO coated fuel particles.

Kinnock V. Munthali,[a,b] Chris Theron[a], F. Danie Auret[a], Sergio M.M. Coelho[a], Linda Prinsloo [a], Eric Njoroge[a]

a.Department of Physics, University of Pretoria
 Pretoria 0002, South Africa
 Phone: +27 124204777
 Fax: +27 123625288

b. Department of Electrical Engineering
   Polytechnic of Namibia
   P/Bag 13388
   Windhoek
   Namibia
   Phone: +264 612072040
   Fax: +264 612072142
   Email: kvmunthali@gmail.com

Abstract

A thin film of ruthenium(Ru) was deposited on n-type 4H-SiC and 6H-SiC by electron beam deposition technique so as to study interface reaction of ruthenium with silicon carbide at various annealing temperatures, and in two annealing environments namely vacuum and air. The Ru-4H-SiC and Ru-6H-SiC films were both annealed isochronally in a vacuum furnace at temperatures ranging from 500 -1000 ^{o}C, and the second set of samples were also annealed in air for temperatures ranging from 100 ^{o}C to 600 ^{o}C. After each annealing temperature, the films were analysed by Rutherford Backscattering spectrometry (RBS). Raman analysis and x-ray diffraction analysis were also used to analyse some of the samples. RBS analysis of 4H-SiC annealed in a vacuum showed evidence of formation of ruthenium silicide (Ru$_2$Si$_3$) and diffusion of Ru into SiC starting from annealing temperature of 700 ^{o}C going upwards. In the case of Ru-6H-SiC annealed in a vacuum, RBS analysis showed formation of Ru$_2$Si$_3$ at 600 ^{o}C, in addition to the diffusion of Ru into SiC at 800 ^{o}C . Raman analysis of the Ru-4H-SiC and Ru-6H-SiC samples that were annealed in a vacuum at 1000 ^{o}C showed clear D and G carbon peaks which was evidence of formation of graphite . As for the samples annealed in air ruthenium oxidation started at a temperature of 400 ^{o}C and diffusion of Ru into SiC commenced at temperatures of 500 ^{o}C for both Ru-4H-SiC and Ru-6H-SiC. X-ray diffraction analysis of samples annealed in air at 600 ^{o}C showed evidence of formation of ruthenium silicide in both 4H and 6H-SiC but this was not corroborated by RBS analysis.

Keywords

1. Introduction

 Silicon carbide (SiC) is used as a layer in tristructural isotropic (TRISO) coated fuel particles in high temperature nuclear reactors. The purpose of TRISO fuel configuration is to act as a containing vessel of actinides and fission products so as to reduce the risk of leakage and coolant contamination [1]. The TRISO coated fuel particle is a microsphere which consists of a fuel kernel surrounded by a buffer layer of low density carbon, followed by layers of inner pyrolytic carbon (IpyC), silicon carbide and outer pyrolytic carbon (OpyC). Each TRISO coating layer has a special function, but SiC is the most important layer that provides most of the structural strength and dimensional stability and acts as the main barrier of metallic fission products. Metals such as ruthenium (Ru), rhodium, palladium, molybdenum, technicium and silver are produced with high yields during fission of uranium and plutonium oxide fuels[1, 2]. Minato et al [3] in their experiments on zirconium carbide Triso-coated uranium dioxide fuel particles found a substantial release of [106]Ru when compared to other released fission products of cesium and europium. Its fraction increased from 0.13 at 1600 ^{o}C for 4500 h to 0.86 at 1800 ^{o}C for 3000 h. Measurements by a gamma ray spectrometer at Chernobyl nuclear disaster area [4] found the existence of Ru radionuclides mainly composed of the following isotopes [103]Ru and [106]Ru .However there is a dearth of literature on the solid state reaction and transport of ruthenium in SiC .

2. Experimental Method

Both n-type 4H-SiC and 6H-SiC from Cree Research were prepared for metallization by degreasing, using an ultra-sonic bath for a period of 5 minutes for each step, in trichloroethylene, acetone and methanol. The samples were deoxidized in 10% HF before rinsing them in deionised water . Nitrogen was used to dry the samples before loading them into the vacuum chamber where 50 nm film of Ru was deposited by e-beam at 10^{-6} mbar pressure. The Ru film thickness was monitored by Infincon meter until the required thickness was obtained. One set of sample was annealed in a furnace vacuum at pressure of less than 10^{-7} mbar for a period of 1 hour for temperatures ranging from 500 ^{o}C to 1000 ^{o}C. Another set of sample was annealed in air in a Lindberg hevi-duty furnace at temperatures ranging from 100 ^{o}C to 600 ^{o}C for 15 minutes. After each annealing temperature Rutherford backscattering spectroscopy (RBS) was used to analyse the samples. Raman spectroscopy and x-ray diffraction (XRD) analysis were also used to analyse some of the samples.

3. Results

3.1. Ruthenium reaction with and diffusion in 4H-SiC and 6H-SiC under vacuum annealing

The RBS spectra for as-deposited Ru-4H-SiC thin film, and samples annealed at 600°C, 700°C and 800°C are shown in Fig.1, Fig. 2, Fig .3 and Fig. 4 respectively. The spectra for annealing temperatures of 900°C and 1000°C were similar to those of the sample annealed at 800°C, and therefore their spectra have not been included in the report. The RBS spectra of the as-deposited sample (Fig.1) and samples annealed at 600 ^{o}C and 800°C (Fig.2 and Fig.3 respectively) were simulated using the RUMP [5] and thereafter converted into depth profiles. The RBS charging current exhibited some instability during the analysis of the sample annealed at 700°C, and therefore its spectrum was not simulated. The as-deposited spectrum displays a pure Ru thin film deposited on 4H-SiC (Fig.1 and Fig.4). After annealing at 600°C, a thin intermixed layer of Ru and Si is observed to form at the interface (Fig.5). The Ru:Si atomic ratio of this layer is found to be 1:1. The carbon released in this case is difficult to observe from the RBS spectra. The raw RBS spectrum for the sample annealed at 700°C (Fig.3) indicates the formation of ruthenium silicide (Ru_2Si_3) as evidenced by the appearance of a step on the high energy edge of Si.

After annealing at a temperature of 800°C, it is observed that the entire deposited Ru layer has reacted with 4H-SiC (Fig.4). From the RUMP simulations (Fig.4, and Fig.7), Si and C can be found on the surface of the sample as these elements are observed at their surface channels of 451 and 184 respectively. The reaction zone is observed to have varying compositions of Ru, Si and C. These ratios vary from a Ru:Si ratio of 1:1 at the surface to 1:6 toward the bulk of the sample.

During the annealing process of the Ru-4H-SiC sample, it is observed from RUMP simulations that Ru diffuses into 4H-SiC, and the dissociated Si and C atoms diffuse into Ru. The reaction zone is observed to grow with increasing annealing temperature. The Ru/4H-SiC interface of the as-deposited sample as depicted in Fig.5 is located 285 x 10^{15} at./cm^2 from the surface of Ru. After annealing at 800°C, Ru is observed to have reacted with 4H-SiC, and Ru is now found 1025 x 10^{15} at./cm^2 from the surface (Fig.7). The step on the high energy edge of Si (Fig.3 and Fig.4), indicates the formation of a Ru_2Si_3. The formation of a silicide and free carbon is corroborated by Raman analysis of the sample.

Fig. 8 is the Raman spectrum obtained at room temperature of Ru-4H-SiC annealed at 1000°C. The spectrum shows the formation of graphite which is evidenced by a clear carbon D peak at 1354 cm^{-1} and a G peak at 1589 cm^{-1} [6, 7, 8, 9, 10, 11] . The intensity ratio of the D and G peaks can be used to approximate the size of the crystalline graphite or degree of disorder of the graphite that is formed [6]. The D band is generally thought to be an indication of disordered or defective hexagonal planar graphite structures. The G band originates from the stretching vibrations in the basal plane of ideal graphite, and a combination of D and G bands is generally regarded as an indication of polycrystalline graphitic structures [7]. The Raman spectrum also shows weak peaks at positions near 500 cm^{-1}, 750 cm^{-1} and 800 cm^{-1}. SiC has Raman peaks called planar E_2 mode, E_1 transverse optic (TO), and A_1 longitudinal optic (LO) mode centred at 777 cm^{-1}, 797 cm^{-1} and 965 cm^{-1} respectively [12, 13, 14, 15] . However for this sample the A_1 peak is very minute. The decrease in intensity of Raman peaks, and the appearance of new spectral bands in SiC, such as peaks near 500 cm^{-1} and 750 cm^{-1}, can be attributed to amorphisation of SiC during the donor implantation process [13]. According to Lu *et al* [8], the absence of a broad amorphous carbon peak at position 1510 cm^{-1} in the Raman spectrum is an indication of the absence (if not the minute presence) of this type of carbon in the sample.

There is also an indication from Raman spectrum of the formation of Ru_2Si_3 as evidenced by the appearance of a peak immediately left of 300 cm^{-1} position [16].
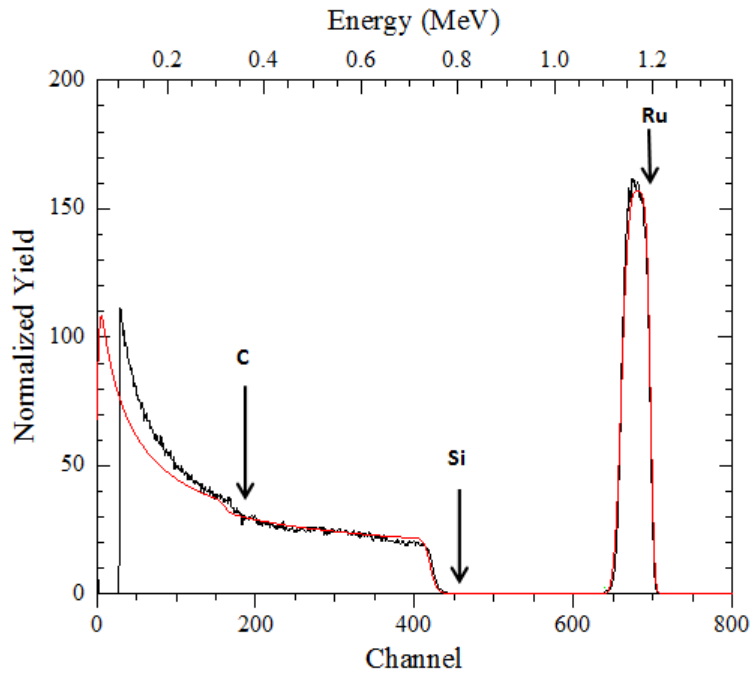

Fig.1.RBS spectra of as-deposited Ru-4H-SiC film where the red and black plots are the simulated and actual profiles respectively.
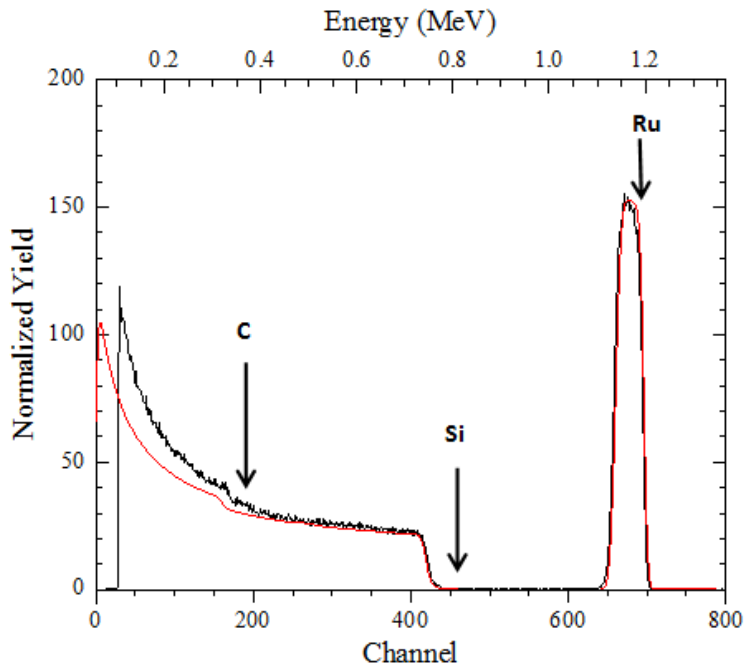

Fig.2. RBS spectra of Ru-4H-SiC film annealed at 600 °C where the red and black plots are the simulated and actual profiles respectively.
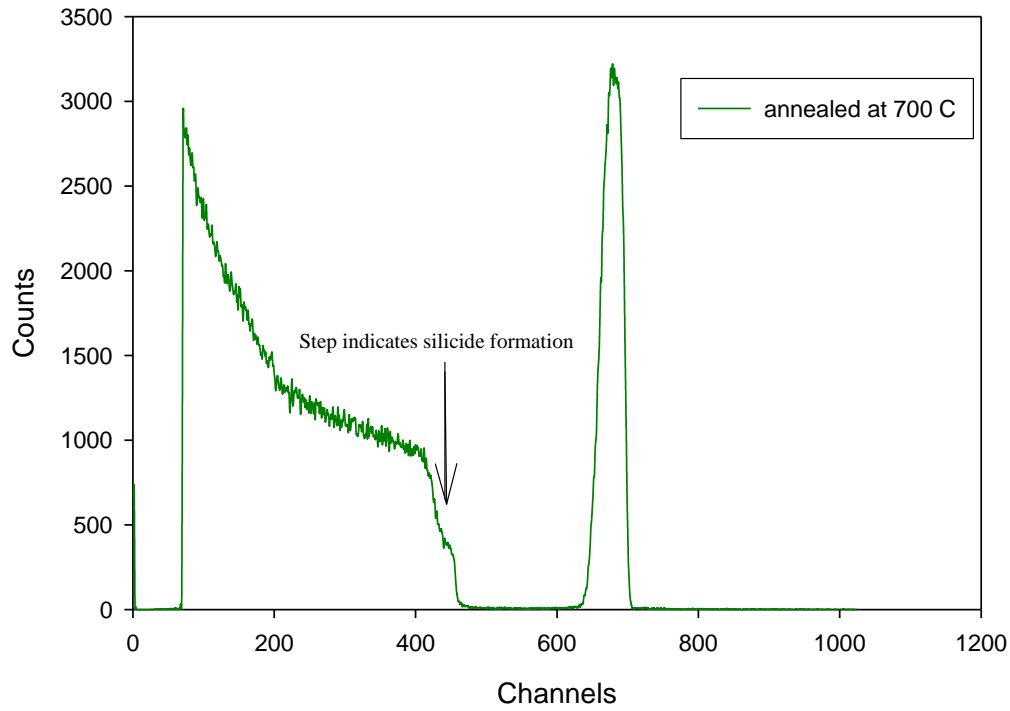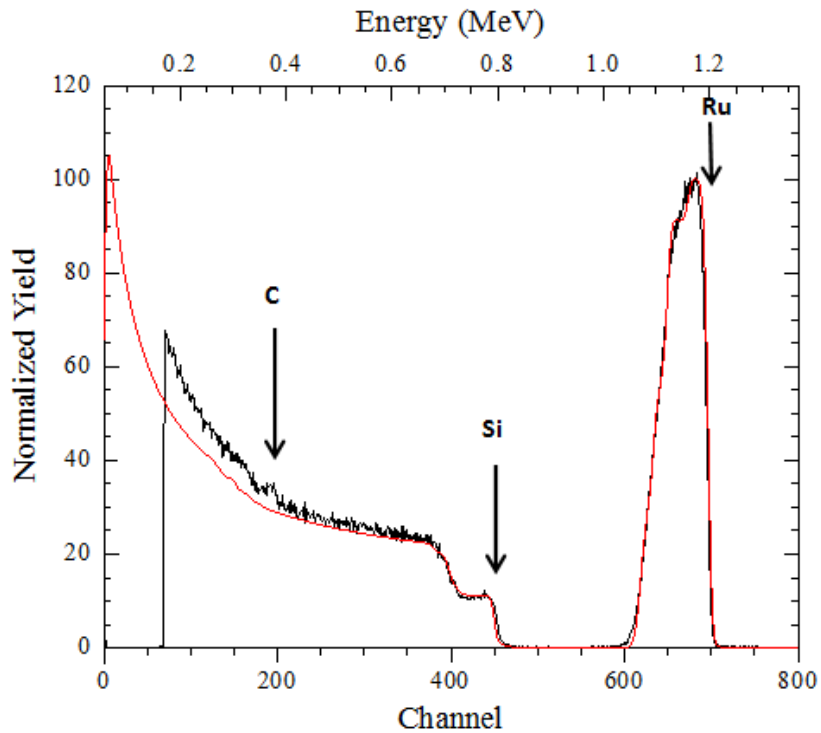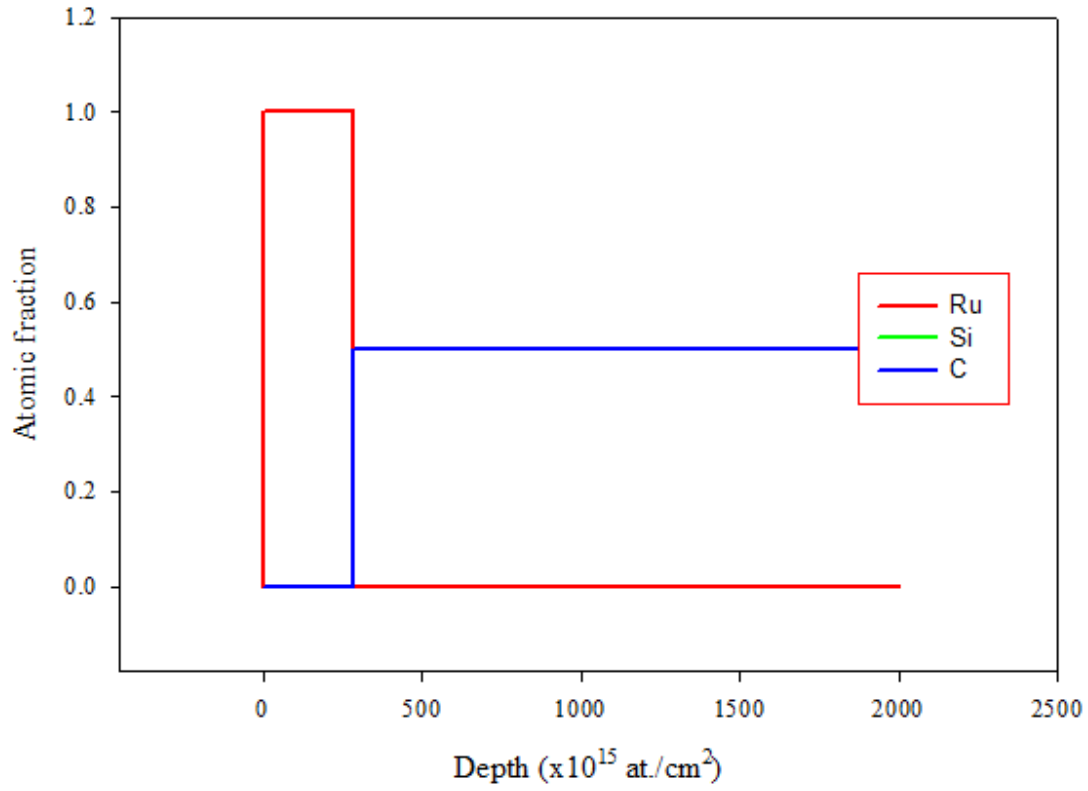
Fig.3. Unnormalised RBS spectra of Ru-4H-SiC annealed in a vacuum at 700 °C

Fig. 4. RBS spectra of Ru-4H-SiC film annealed at 800 °C where the red and black plots are the simulated and actual profiles respectively.
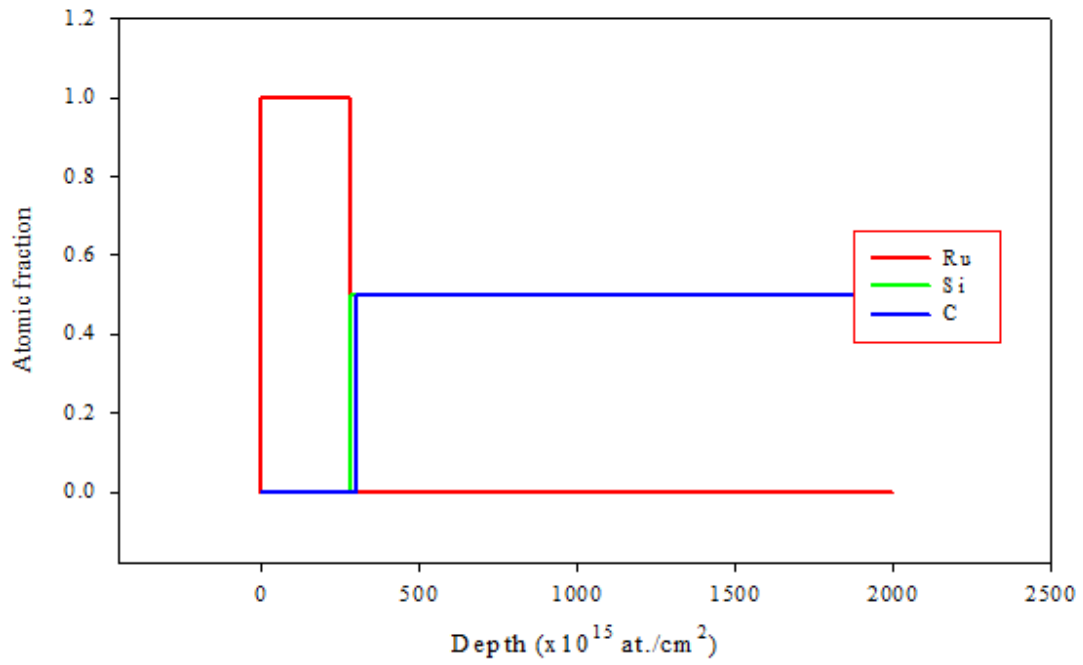
Fig.5. Depth profile of as-deposited Ru-4H-SiC

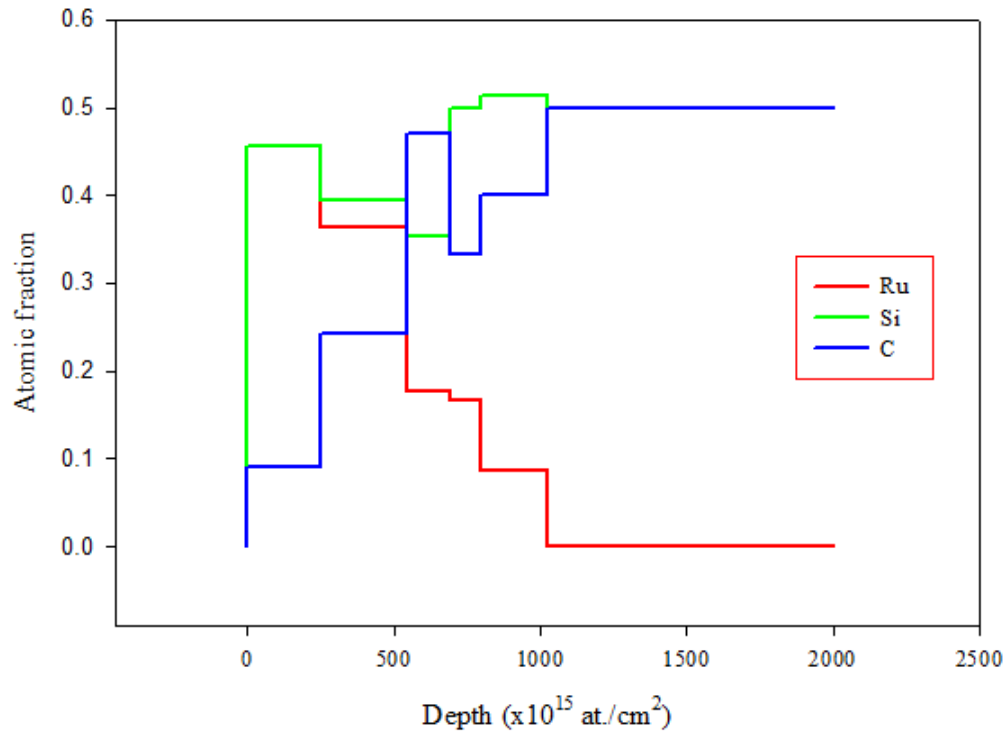Fig. 6. Depth profile of Ru-4H-SiC annealed in a vacuum at 600 C.

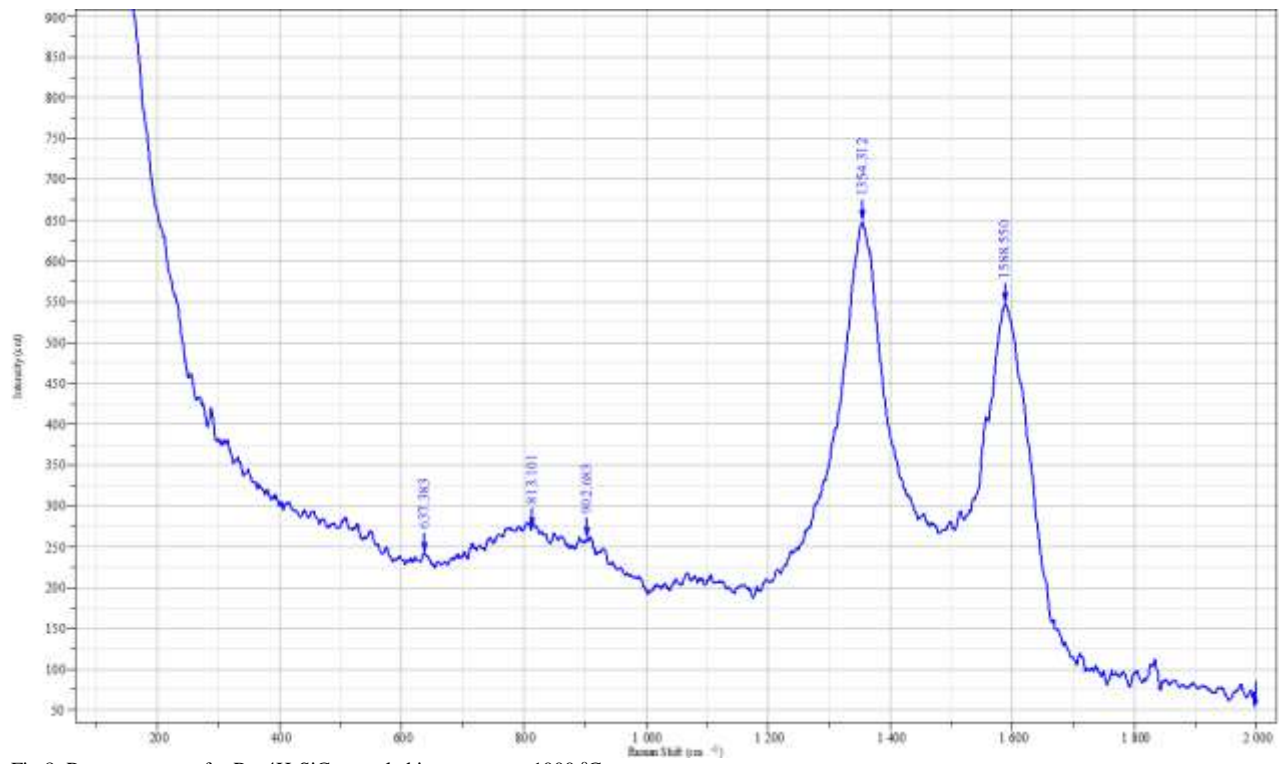Fig. 7. Depth profile of Ru-4H-SiC annealed in a vacuum at 800 C.

Fig.8. Raman spectra for Ru-4H-SiC annealed in vacuum at 1000 °C.

The as-deposited RBS spectrum of Ru-6H-SiC (not shown) is similar to the sample annealed at 500 $^{\circ}$C in a vacuum (Fig. 9). There is indication of Ru$_2$Si$_3$ formation at 600 $^{\circ}$C as evidenced by the presence of a step near the high energy step of Si (Fig.10). The silicide formation is more pronounced at annealing temperature of 1000 $^{\circ}$C as indicated by steps on the high energy edge of Si and low energy edge of Ru (Fig.12). Diffusion of Ru into SiC commences at 800 $^{\circ}$C (not shown), and is more pronounced at 900 $^{\circ}$C as indicated by a very wide bottom of Ru signal (Fig.11). Plots of depth profiles (Fig.13 and Fig. 14) have been obtained from RUMP simulations. From these simulations, it is observed that Ru diffuses into 6H-SiC, and the dissociated Si and C atoms also diffuse into Ru. The reaction zone increases with annealing temperature. The Ru/6H-SiC interface of the as-deposited sample (Fig.13) is located 320x 10^{15} at./cm^2 from the surface of Ru. Ru is observed to react with 6H-SiC, and is found at 2300 x 10^{15} at./cm^2 from the surface (Fig.14) after annealing at 1000°C.

Raman spectrum of Ru-6H-SiC annealed in a vacuum at 1000 $^{\circ}$C (Fig. 15) clearly indicates the formation of graphitic structures as evidenced by the D and G carbon peaks at 1356 cm^{-1} and 1589 cm^{-1} respectively [6, 7, 8, 9, 10, 11].

These findings indicate that ruthenium as a fission product in TRISO coated fuels is able to diffuse through the 6H-SiC layer at temperatures of 800 $^{\circ}$C and above.

Fig 9. RBS spectra of Ru-6H-SiC annealed in a vacuum at 500°C obtained by using 1.4 MeV of helium ions. The black and red plots are actual and simulated profiles respectively.
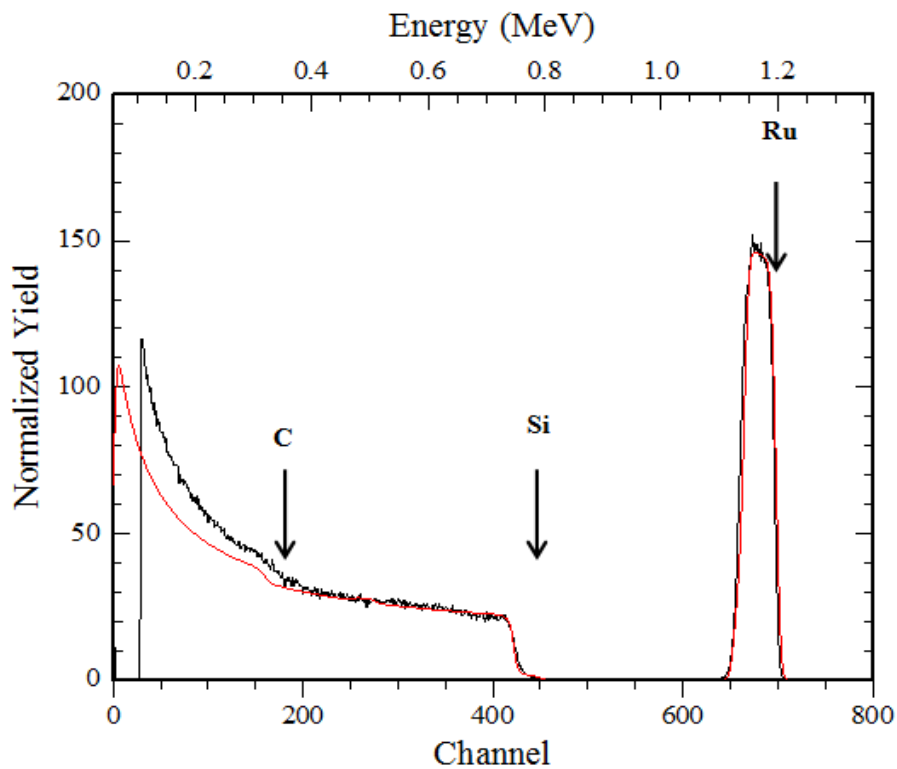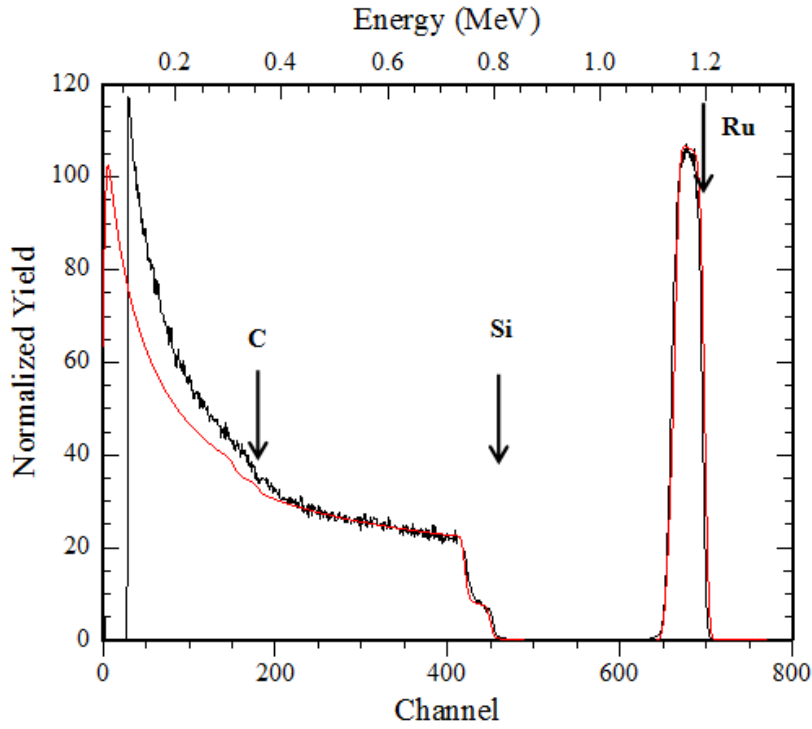
Fig 10. RBS spectra of Ru-6H-SiC annealed in a vacuum at 600ºC obtained by using 1.4 MeV of helium ions. The black and red plots are actual and simulated profiles respectively.
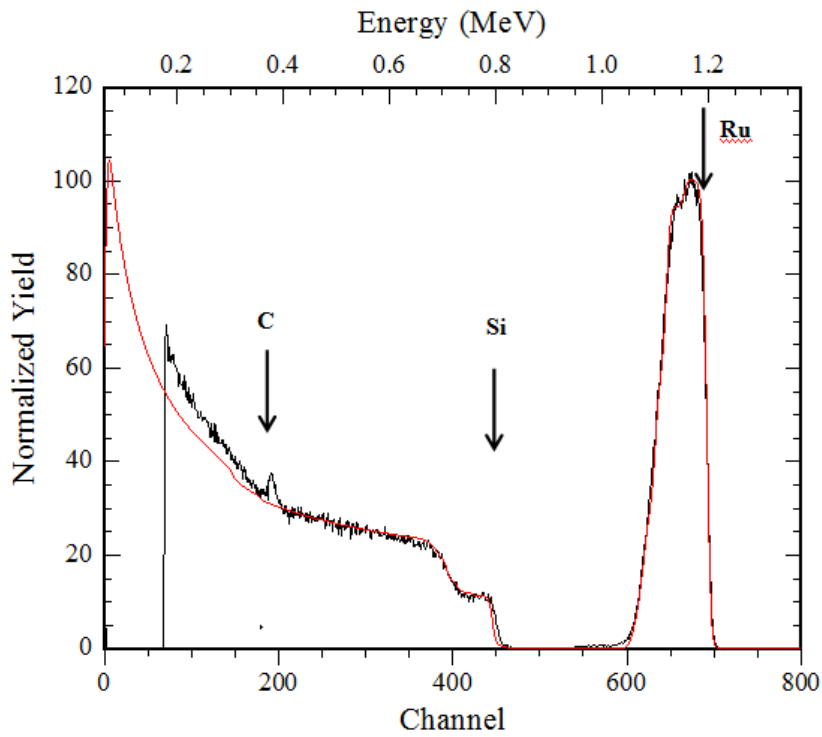

Fig.11. RBS spectra of Ru-6H-SiC annealed in a vacuum at 900ºC obtained by using 1.4 MeV of helium ions. The black and red plots are actual and simulated profiles respectively.
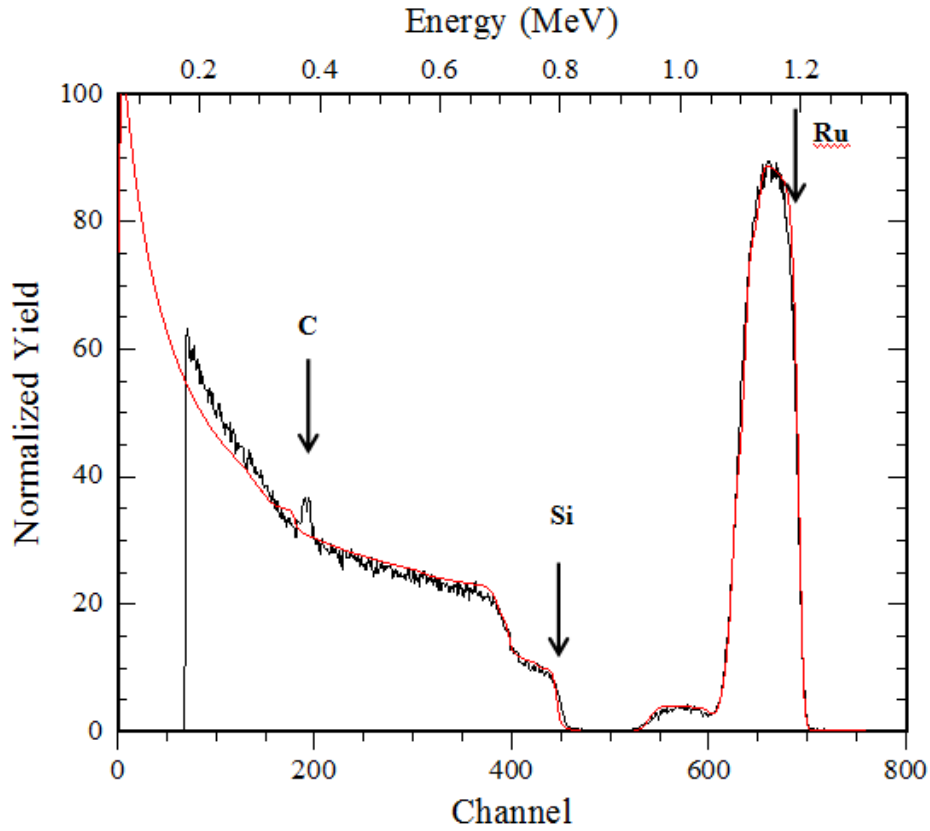
Fig.12. RBS spectra of Ru-6H-SiC annealed in a vacuum at 1000ºC obtained by using 1.4 MeV of helium ions. The black and red plots are actual and simulated profiles respectively.
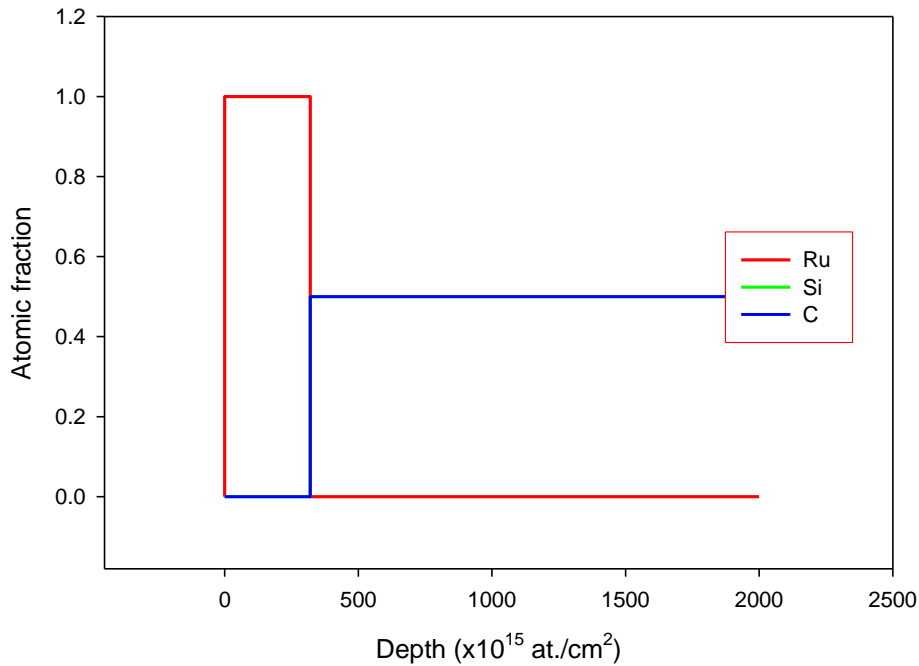

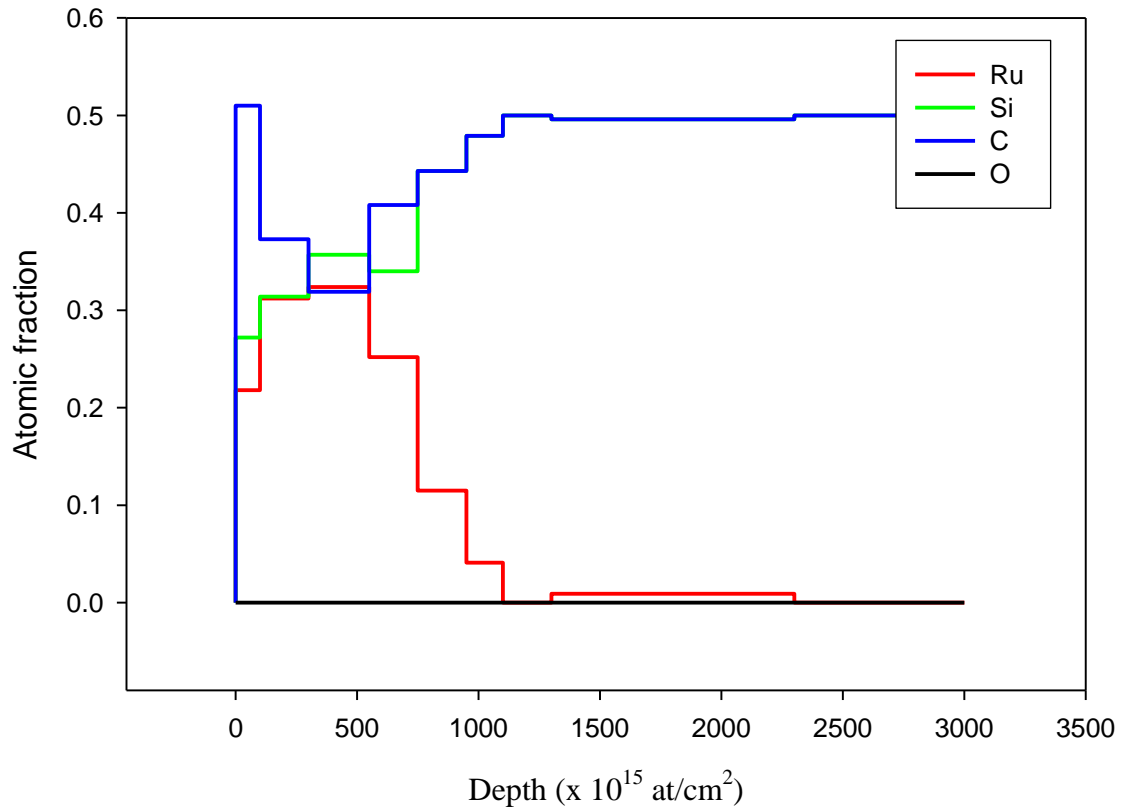Fig. 13. Depth profile of as-deposited Ru-6H-SiC

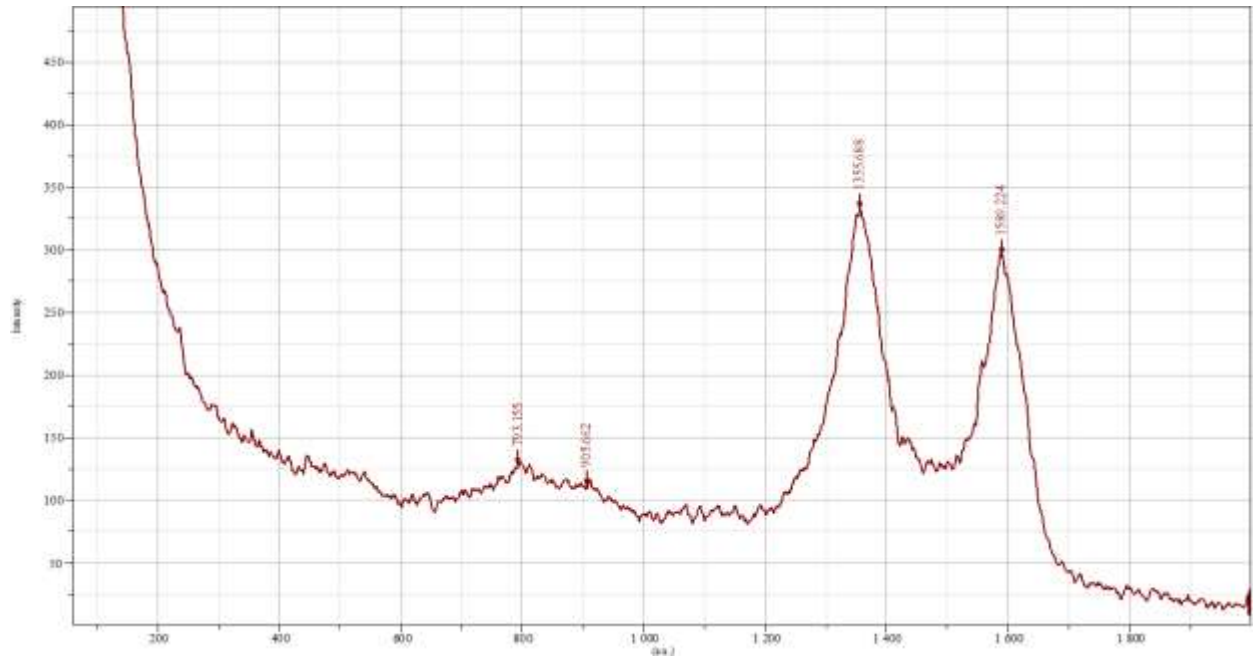Fig. 14. Depth profile of Ru-6H-SiC annealed at 1000 ^{o}C in a vacuum.

Fig 15. Raman spectrum of Ru-6H-SiC film annealed in vacuum at 1000 ^{o}C .

3.2. Ruthenium reaction with and diffusion in 4H-SiC and 6H-SiC when annealed in air

The as-deposited Ru-4H-SiC displays a pure ruthenium on the surface of the sample (Fig. 16). The RBS spectra of Ru-4H-SiC sample in Fig.17 reveals that oxidation of ruthenium begins at annealing temperature of 400 ^{o}C as seen by a the presence of an oxygen peak at channel number 178. The oxygen peak is more pronounced for the sample annealed at 500 ^{o}C (Fig.18) .There is a heavy suspicion that the resulting oxide is not the semiconducting oxide RuO_2 but other oxides compounds such as gaseous RuO and low temperature melting RuO_4 or RuO_3 which is known to vaporise at 1200 ^{o}C or Ru_2O_3 which is largely unknown[17, 18]. From the Raman spectra of the sample annealed at 600 ^{o}C (Fig. 20), there is a clear absence of RuO_2 peaks [19] which is an indication of the absence of the ruthenium oxide with this stoichiometry. In stead there is a clear Ru_2Si_3 peak at position 203 cm$^-$^{1}[20], and typical three main phonon bands of 4H-SiC with A1, and E2 symetries [21] . The planar E2, transverse optic E1 and the longitudinal optic A1 modes are at positions 776 cm^{-1}, 797 cm^{-1} and 964 cm^{-1} respectively.

Depth profiles of Ru-4H-SiC which were obtained from RUMP simulations of RBS spectra indicate surface oxidation at 400 ^{o}C (Fig. 21) and ruthenium diffusion into 4H-SiC (Fig. 22) at 500 ^{o}C. From the RBS spectra diffusion is more pronounced at 600 ^{o}C(Fig. 19). X-ray diffraction (XRD) analysis of a Ru-4H-SiC thin film sample annealed at 600 ^{o}C (Fig. 23) indicates the formation of ruthenium silicide but this is not corraborated by RBS analysis .
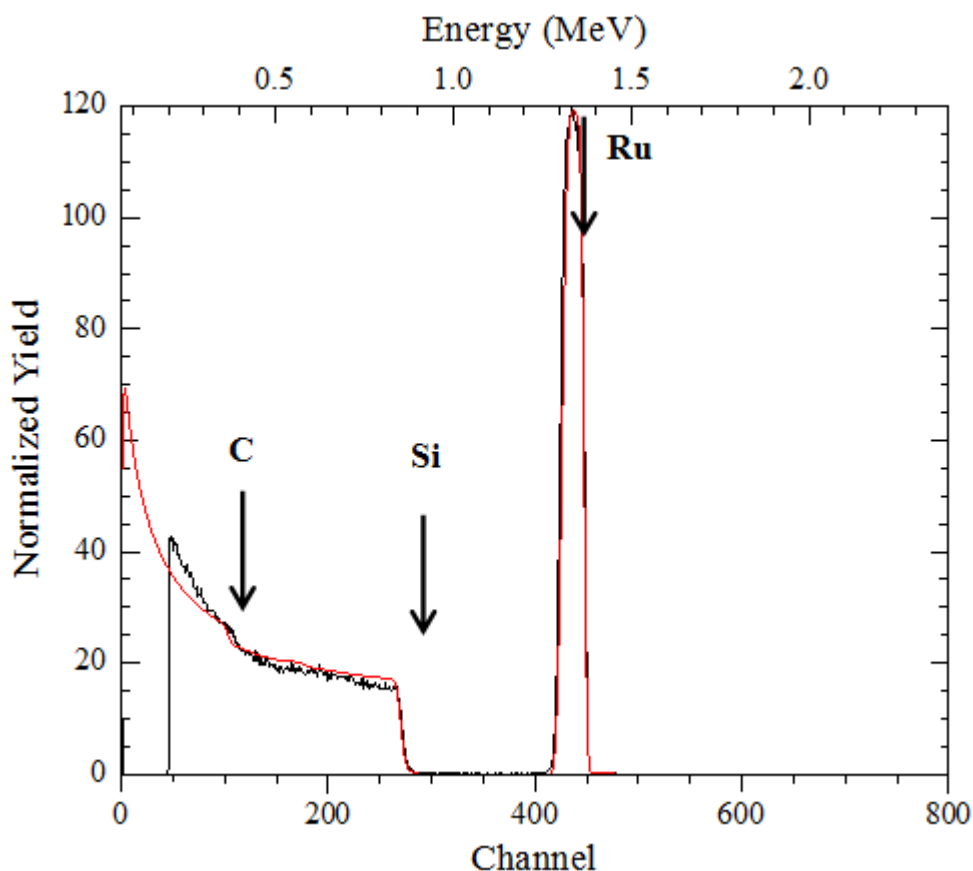

Fig.16. RBS spectra of as-deposited Ru-4H-SiC obtained by using 1.6 MeV of helium ions. The black and red plots are actual and simulated profiles respectively.
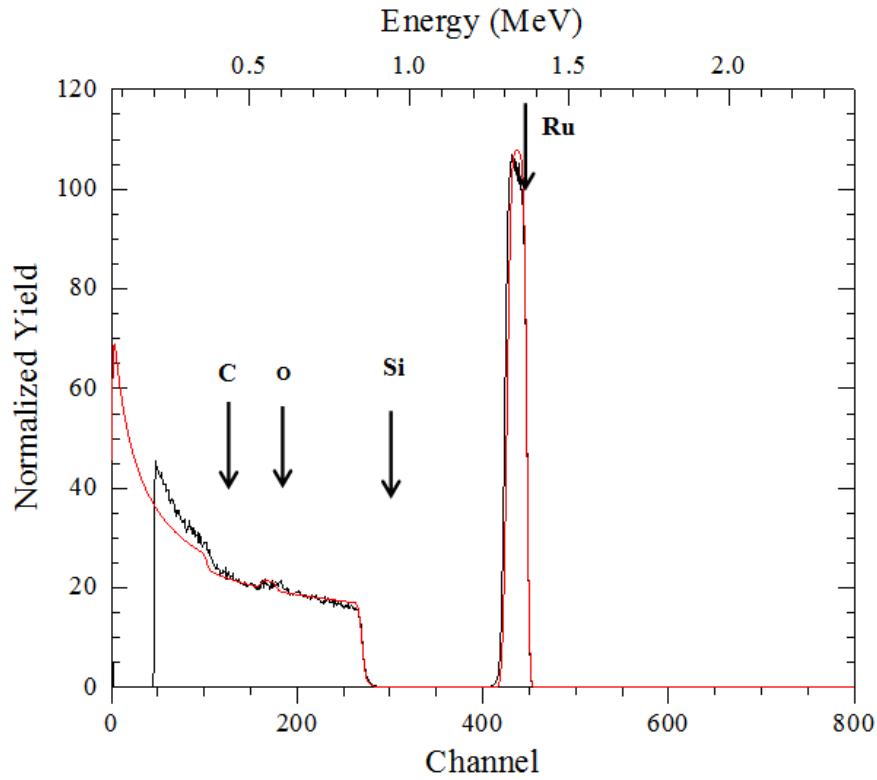
Fig.17. RBS spectra of Ru-4H-SiC annealed in air at 400ºC obtained by using 1.6 MeV of helium ions. The black and red plots are actual and simulated profiles respectively.
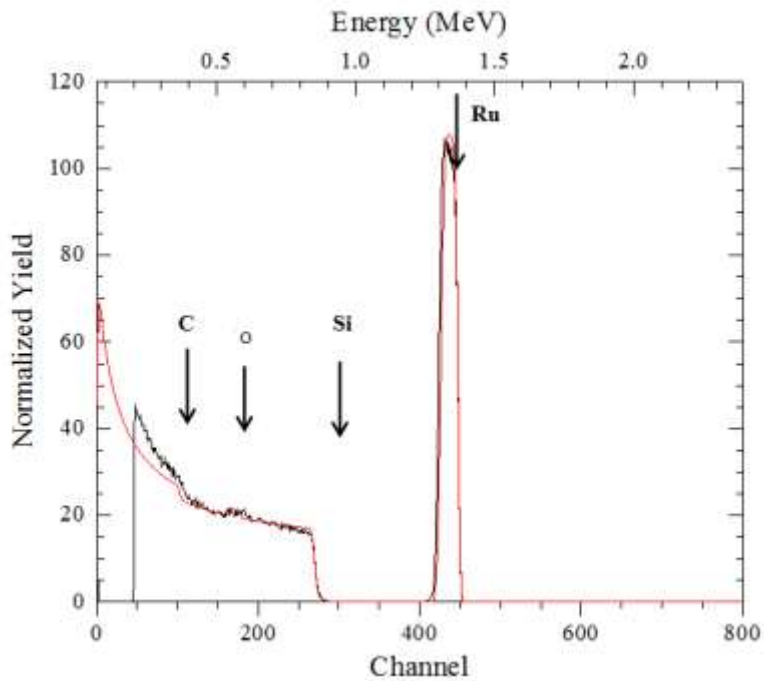

Fig.18. RBS spectra of Ru-4H-SiC annealed in air at 500ºC obtained by using 1.6 MeV of helium ions. The black and red plots are actual and simulated profiles respectively.
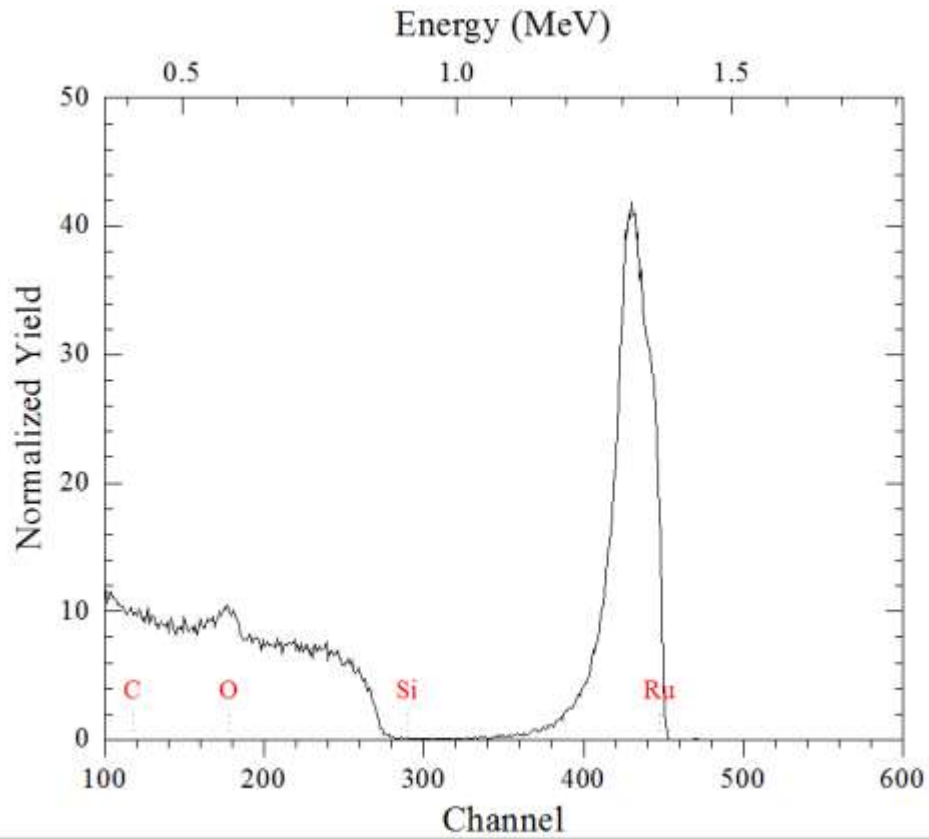
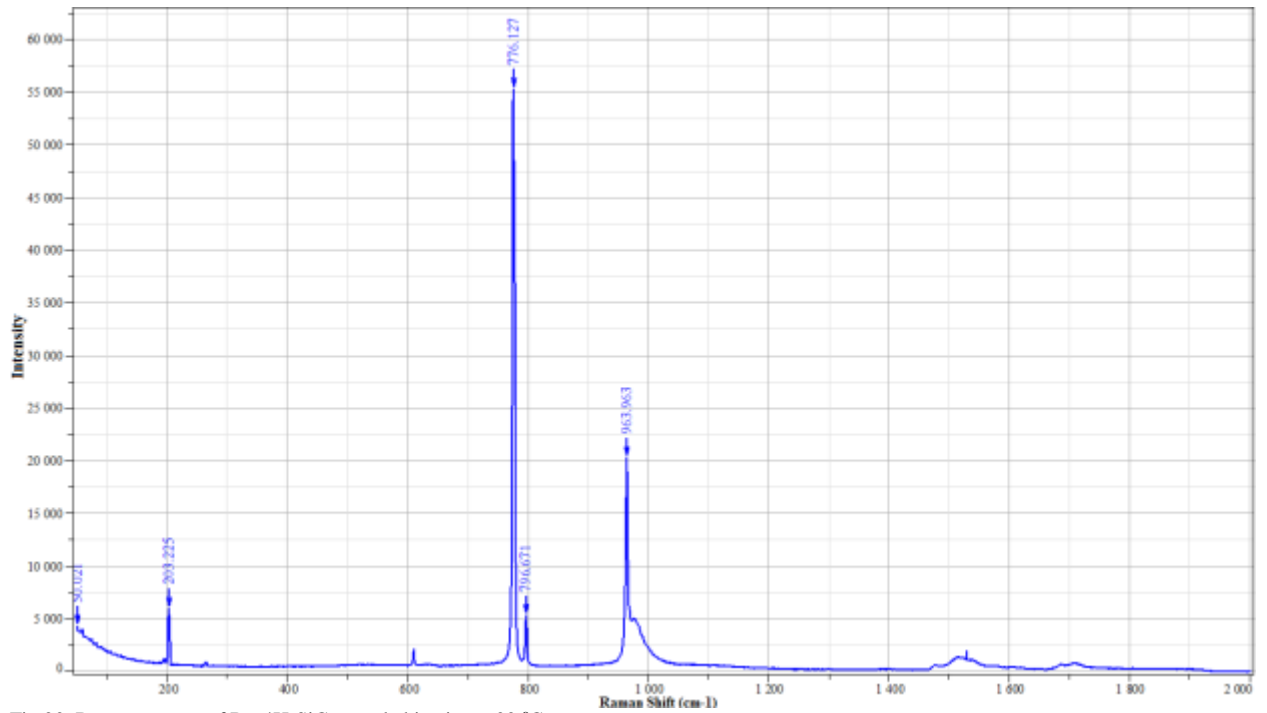Fig.19. RBS spectra of Ru-4H-SiC annealed in air at 600°C obtained by using 1.6 MeV of helium ions.

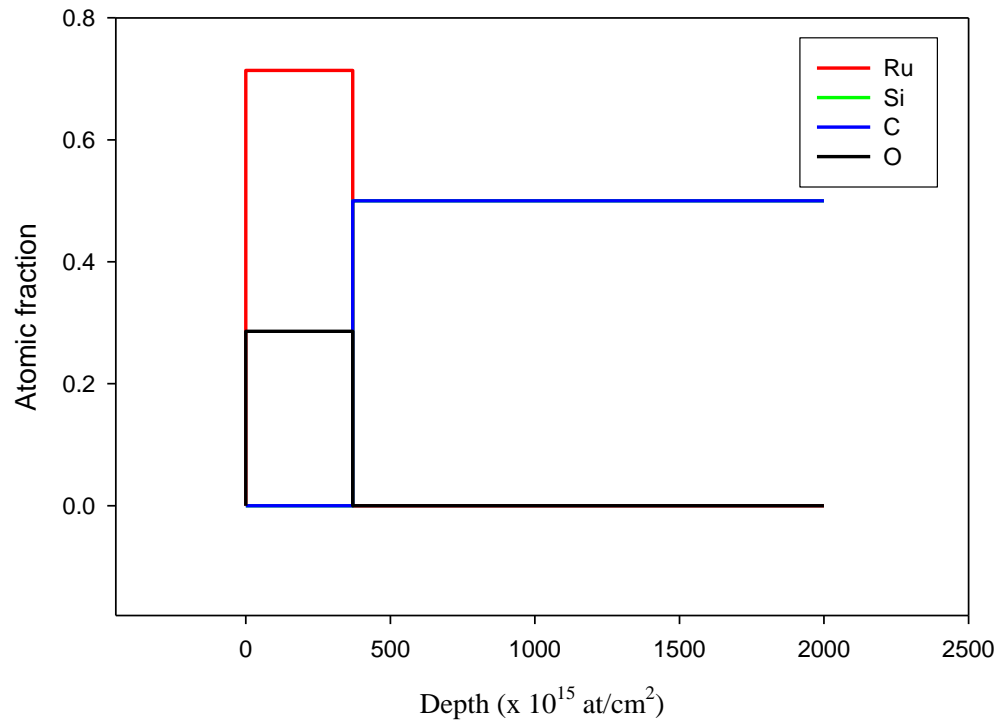Fig 20. Raman spectra of Ru-4H-SiC annealed in air at 600 °C.

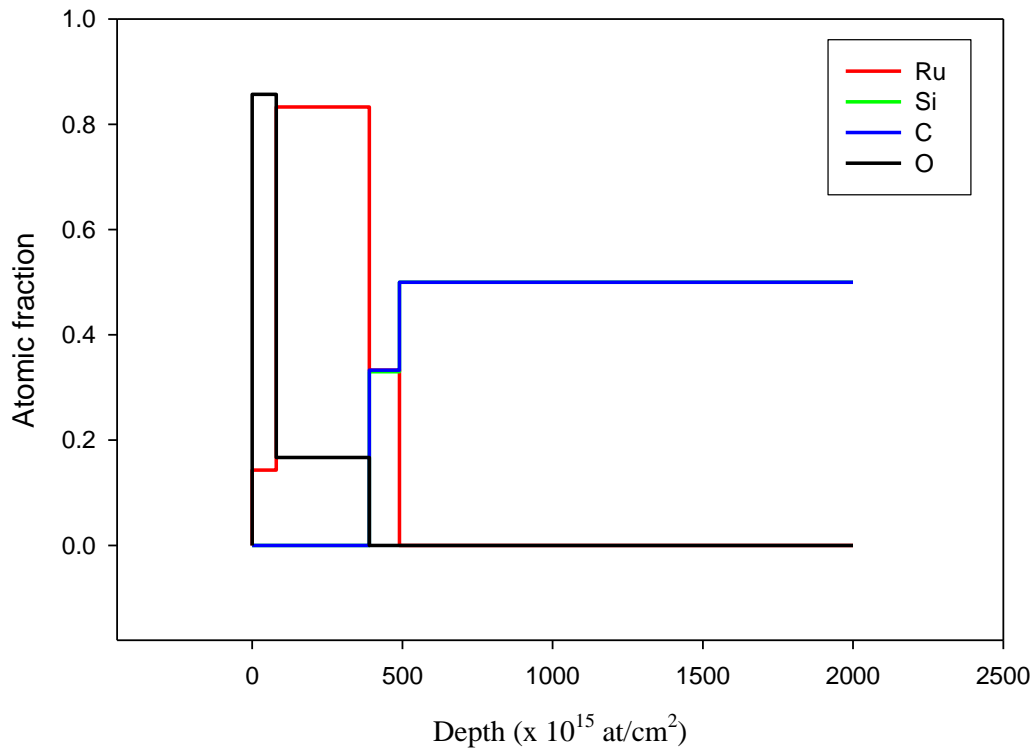Fig 21. Depth profile of Ru-4H-SiC annealed in air at 400 ºC.

Fig. 22. Depth profile of Ru-4H-SiC annealed in air at 500 ºC.
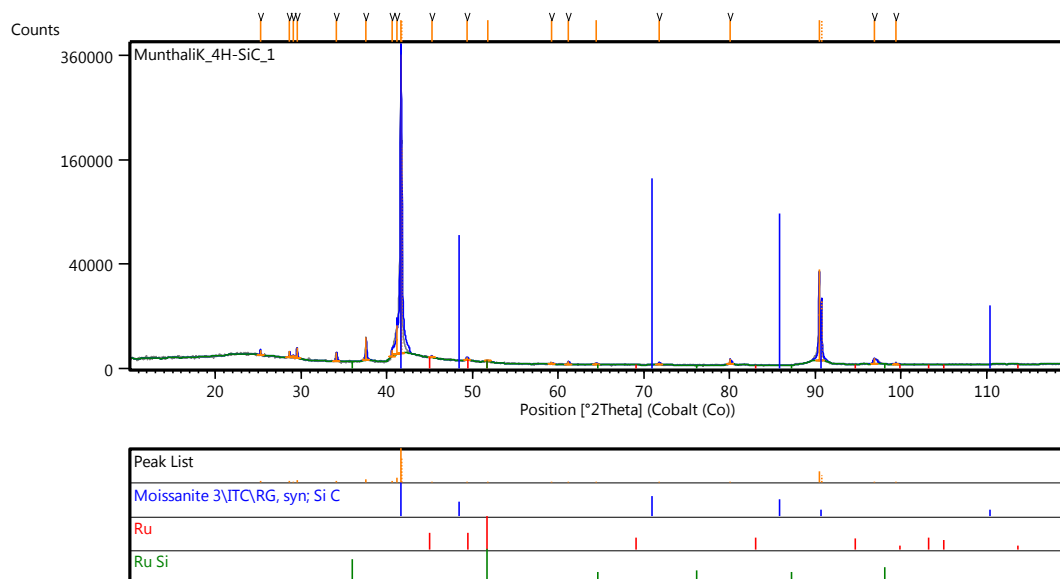
Fig 23. XRD spectra of Ru-4H-SiC annealed in air at 600 °C.

RBS analysis of Ru-6H-SiC annealed in air indicates oxidation at a low temperature of 400 °C (not shown) , and inter-diffusion of Ru and Si after annealing temperatures of 500 °C (Fig. 24) . At 600 °C the diffusioon of Ru into SiC is very deep as indicated by the joining of the Ru and Si signals (Fig. 25). What can be noted is this study is that diffusion of Ru into 6H-SiC commences at a much lower temperature under atmospheric annealing than under vacuum annealing.

 The analysis of XRD spectrum using X'Pert Highscore plus software   indicated the formation of RuO_2 and RuSi (Fig. 26) at an annealing temperature of 600 °C. Raman spectrum of Ru-6H-SiC annealed at 600 °C in air (Fig. 27) clearly shows the typical Raman bands of RuO_2 at positions 524, 643 and 710 cm^{-1}[19].

Fig .24. RBS spectra of Ru-6H-SiC annealed in at 500 °C obtained by using 1.6 MeV helium ions.

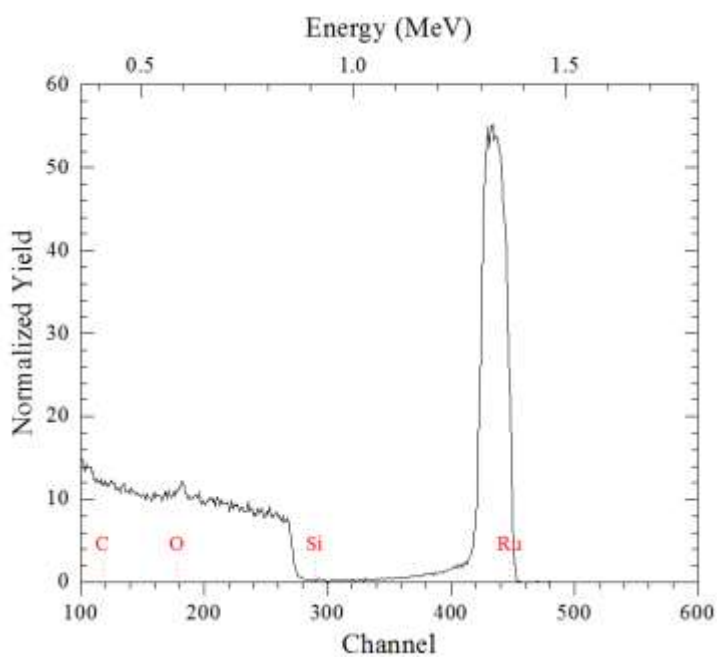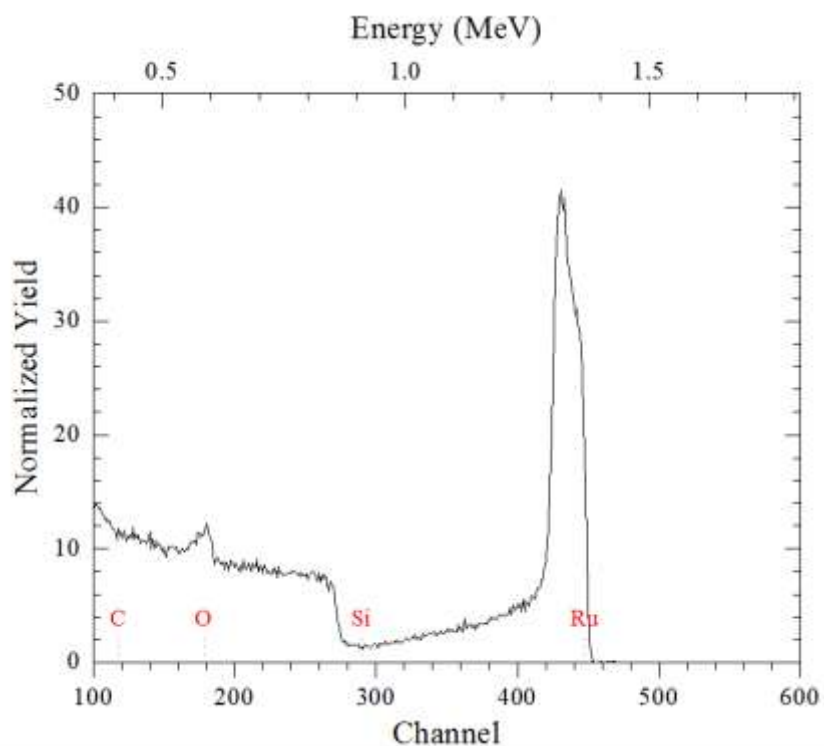Fig .25. RBS spectra of Ru-6H-SiC annealed in at 600 ºC obtained by using 1.6 MeV helium ions.
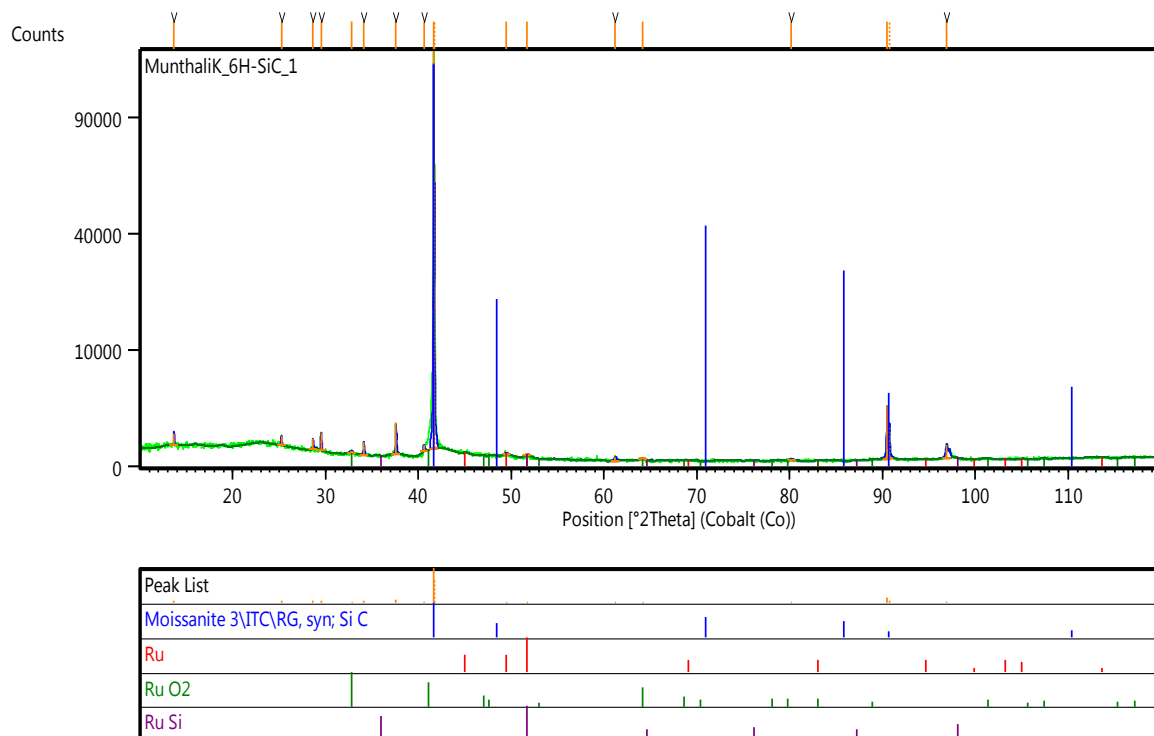

Fig. 26. XRD spectrum of Ru-6H-SiC thin film sample annealed in air at 600 ºC.
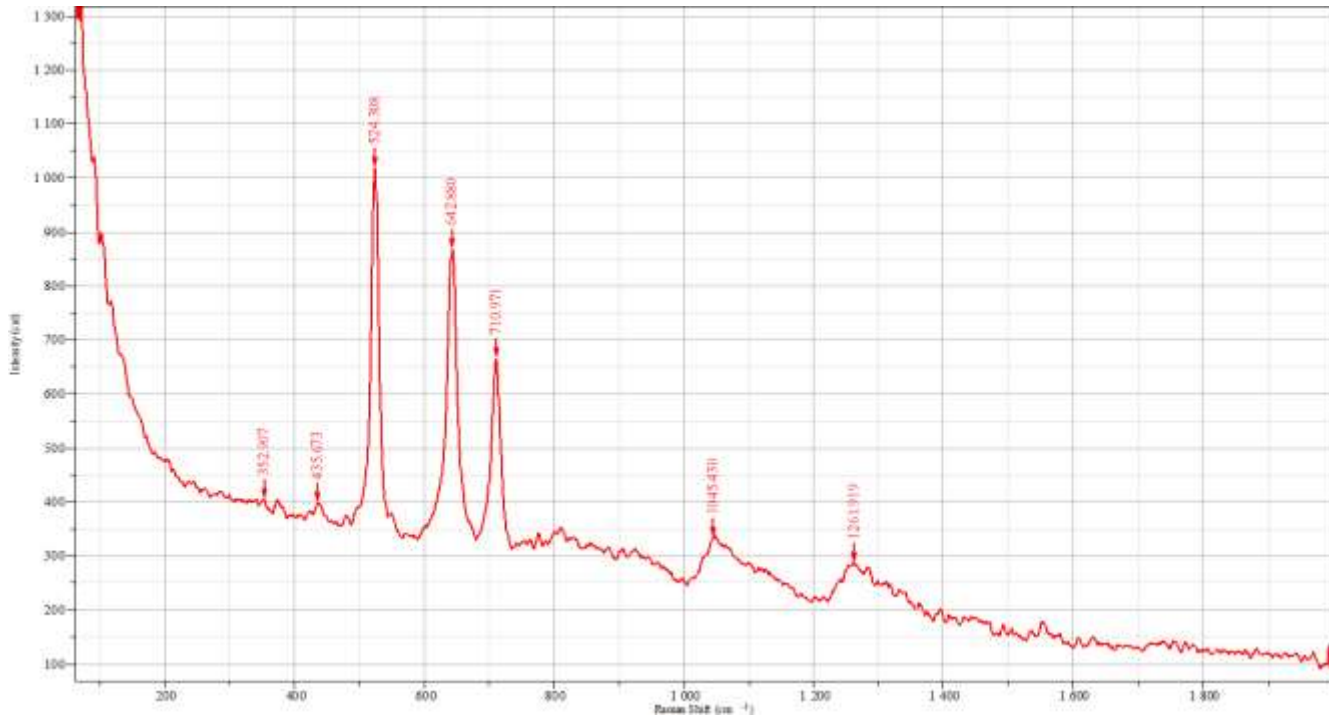
Fig. 27. Raman spectrum of Ru-6H-SiC thin film sample annealed in air at 600 $^{\circ}$C.

4. Discussion

This study has shown that there is diffusion of Ru into 4H-SiC and 6H-SiC under vacuum anneling and air annealing. Diffusion of Ru starts at a much lower temperature for both SiC polytypes under air annealing as compared with vacuum annealing. The results have also shown that both polytypes undergo silicidation under vacuum annealing, and that there is formation of ruthenium oxide under air annealing. In actinide oxide fuels, oxygen is released in the fission reaction [1] and therefore will react with Ru as has been demonstrated in this study.

Now, what important information can be gleaned from this study which will shed light on the integrity of SiC as a diffusion barrier to fission products in TRISO particles? Let us first outline some differences between this diffusion study experiment and the actual process of burn-up in TRISO particles. In TRISO particles the concentration of ruthenium on the SiC surface is likely to be lower than in this thin film experiment, and consequently the reaction penetration depth into SiC should be lower as well. Experiments have shown that the rate-limiting step in fission product palladium (Pd) attack on SiC depends on the supply of Pd from the kernel and and the rate of diffusion of Pd through the buffer and inner PyC layer [22]. According to Sawa et al [22], studies of interaction of Pd with SiC have shown that the maximum reaction depth will depend on the amount of Pd released from the kernels. The penetration depth has been shown to be directly proportional to the cube root of concentration of Pd. The maximum penetration depth for the fuel lifetime has been calculated to be 11 μm which is less than half of the SiC layer thickness. Since Ru just like Pd belong to the platinum metal groups , and has similar chemical and physical characteristics, the expectation is that the diffusion depth should closely mirror that of Pd.

The other difference between the thin film experiment in this study and TRISO particles is that during burn-up of TRISO particles, extreme pressure is created in the coated fuel particle due to the formation of fission gases such as xenon and krypton. The amount of fission gases released from the kernel of a TRISO particle depends on temperature, burnup and time [23]. Experiments have shown that as burn-up increases, there is a concomitant increase in presure and temperature in the fuel particle. Metallic fission product release is usually modeled by Fickian diffusion with Arrehnius diffusion coefficients, and from this modeling, diffusion is shown to be a function of time and temperature . From this information, we can conclude that extreme pressure will increase the rate of diffusion of fission metals.

In UO$_2$ fuel particles, the fission reaction produces a net excess of free oxygen as the fission products that are produced do not consume all the oxygen that is realeased [23]. This is due to the fact that the thermo-chemical conditions are unfavourable for these fission metals to form stable oxides[2].This excess oxygen reacts with the buffer to form CO gas which greatly increases

the internal pressure in the particle. This CO may break into the PyC layer, and then react with SiC to form SiO. The breaking of the PyC layer by CO will enhance the diffusion of fission metal products such as Ru which will react with SiC as well as oxygen. Some authors [24] have argued that there is a possibility of introduction of defects in the SiC crystal through the incorporation of the fission product Ru and oxygen into the crystal under some favourable oxygen partial pressure .The introduction of the defects will increase the diffusion of the fission metal product through the crystal. The thin-film air annealing experiment in this study directly mirrors this situation. The study has shown that diffusion of Ru into SiC starts at a lower temperature in air annealing as compared to vacuum annealing.

The SiC layer in TRISO particles is commonly deposited by a chemical-vapour-deposition (CVD) process, and the resulting SiC is the cubic β-SiC. The physical and chemical properties of β-SiC are very similar to those of 4H-SiC and 6H-SiC used in this experiment. The only difference among these three SiC polytypes is the arrangement of the Si-C atomic planes. The point that is getting emphasized here is that the results obtained in this study are applicable to the CVD SiC used in TRISO fuel particles. Moreover studies have shown that β-SiC transforms to α-SiC at temperatures between $1600\,^{o}$C to $2000\,^{o}$C [2]. The authors intended to anneal up to temperatures above $1000\,^{o}$C, but the constraint was that the vacuum furnace had a maximum annealing temperature of $1000\,^{o}$C. However some high temperature gas-cooled reactors (HTGR) operate at temperatures of around $950\,^{o}$C [2], so the results in this study will be directly applicable to such reactors. Furthermore from having a fore knowledge that diffusion of fission products is a function of time and temperature, and having established in this study that there is Ru diffusion in SiC beginning from a lower temperatures of $500\,^{o}$C and up to a maximum annealing temperature of $1000\,^{o}$C in very low annealing times of 15 minutes and 1 h, the extrapolation is that there will be increased diffusion if the temperatures are increased above $1000\,^{o}$C and the annealing time increased to more than 1 year as normally happens in actual irradiation in high temperature nuclear reactors.

5. Conclusion

It has been shown in this paper that there is solid state diffusion of Ru in both 4H-SiC and 6H-SiC thereby showing that SiC is not a perfect barrier to metallic fission products in TRISO coated fuel particles. The study has demonstrated that diffusion of Ru into SiC starts at a much higher annealing temperature ($700\,^{o}$C and $800\,^{o}$C for 4H-SiC and 6H-SiC respectively) in a vacuum, whereas in air annealing diffusion commences at a much lower temperature of $500\,^{o}$C. The experimental data has also shown that there is oxidation of ruthenium in air annealing. What can be noted is that in nuclear oxide fuels, oxygen is released in fission reaction and from these results, an inference can be made that the fission product Ru can be expected to start diffusing through SiC at a much lower temperature.

This study has also shown that the formation of ruthenium oxide , ruthenium silicide, graphite and the commencement of diffusion of Ru into SiC depend on three factors namely; annealing temperature, annealing environment and polytype of SiC.

6. References

[1] T.M. Besmann, R.E. Stoller , G. Samolyuk, P.C. Schuck , S.I. Golubov , S.P. Rudin , J.M. Wills ,J.D. Coe , B.D. Wirth , S. Kim , D.D. Morgan , I. Szlufarska , Journal of Nuclear Materials 430 (2012) 181-189.
[2] X.W. Zhou, C.H. Tang, Progress in Nuclear Energy 53 (2011) 182-188.
[3] K. Minato, T. Ogawa, T. Koya, H. Sekino, T. Tomita, Journal of Nuclear Materials 279, (2000) 181-188 .
[4] R. Pollanen, Radiation Protection Dosimetry vol. 71 No.1, pp. 23-32 (1997).
[5] L.R. Dolittle, Nuclear Instruments and Methods, B9, p. 344 (1985).
[6] Z. Juang, C. Wu, C. Lo, W. Chen, C. Huang, J. Hwang, F. Chen, K. Leou, C. Tsai, Carbon, vol. 47, (2009) 2026 −2031.
[7] V. Mennella, G. Monaco, L. Colangeli, E. Bussoletti, Carbon vol 33, No. 2, (1995) 115-121.
[8] W. Lu, W.C. Mitchel, C.A. Thornton, G.R. Landis, W.E. Collins, Journal of Electronic Materials, Vol. 32, No.5(2003).
[9] H. Hiura, T.W. Ebbesen, K. Tanigaki, Chemical Physics Letters vol 202, number 6, (1993).
[10] P.C. Eklund, J.M. Holden, R.A. Jishi, Carbon vol. 33, No. 7 (1995). 959-972.
[11] A.C. Ferrari, Solid State Communications, 143, (2007) 47-57.
[12] M. Chafai, A. Jaouhari, A. Torres, R. Anton, E. Martin, J. Jimenez, W.C. Mitchel, Journal of Applied Physics , vol 90, Number 10.
[13] A. Perez-Rodriguez, Y. Pacud, L. Calvo-Barrio, C. Serre, W. Skorupa, J.R. Morante, Journal of Electronic Materials, Vol. 25, No.3, (1996).
[14] S. Nakashima, Y. Nakatake, H. Harima, M. Katsuno, N. Ohtani, Applied Physics Letters, Vol. 77, No.22, (2000).
[15] M. Wieligor, Y. Wang, T.W. Zerda, Journal of Physics: Condensed Matter, 17, (2005) 2387-2395.
[16] E.V. Jelenkovic, K.Y. Tong, W.Y. Cheung, S.P. Wong, Semiconductor Science Technology, 18, (2003) 454-459
[17] Jelenkovic E.V, Tong K .Y, Cheung W. Y, Wong S. P, Semiconductor Science Technology 18, (2003) 454-459.
[18] M.M. Steeves, Electronic transport properties of ruthenium and ruthenium oxide thin films, A PhD thesis, (unpublished results).
[19] E.V. Jelenkovic, K.Y. Tong, Journal of Vacuum Science Technology B 22(5), (2004).

[20] A.G. Birdwell, Optical properties of β-FeSi$_2$, Ru2Si$_3$, and OsSi$_2$: semiconducting silicides, PhD Thesis (unpublished results).

[21] M. Chafai, A. Jaouhari, A. Torres, R. Anton, E. Martin, J. Jimenez, W.C. Mitchel, Journal of Applied Physics , vol 90, Number 10.

[22] K. Sawa, S. Ueta, Nuclear Engineering and Design 233, (2004) 163-172.

[23] J.T. Maki, D.A. Petti, D.A. Knudson, G.K. Miller, Journal of Nuclear Materials 371, (2007) 270-280.

[24] A. Londono-Hurtado, A.J. Heim, S. Kim, I. Szlufarska, D. Morgan, Journal of Nuclear Materials 439, (2013) 65-71.